Available online at www.sciencedirect.com
SCIENCE DIRECT®
Journal of Power Sources 125 (2004) 52–61
JOURNAL OF POWER SOURCES
www.elsevier.com/locate/jpowsour

Heat transfer characteristics of the metal hydride vessel based on the plate-fin type heat exchanger

Tsutomu Oi [a,*], Kohei Maki [a], Yoshinori Sakaki [b]

[a] *Shinko Pantec Co. Ltd., 1-1-4 Murotani, Nishi-ku, Kobe 651-2241, Japan*
[b] *Chubu Electric Power Co. Inc., 20-1 Azakitasekiyama, Ohdaka-cho, Midori-ku, Nagoya 459-8522, Japan*

Received 28 May 2003; received in revised form 25 June 2003; accepted 16 July 2003

Abstract

Heat transfer characteristics of the metal hydride vessel based on the plate-fin type heat exchanger were investigated. Metal hydride beds were filled with AB_2 type hydrogen-storage alloy's particles, $Ti_{0.42}Zr_{0.58}Cr_{0.78}Fe_{0.57}Ni_{0.2}Mn_{0.39}Cu_{0.03}$, with a storage capacity of 0.92 wt.%. Heat transfer model in the metal hydride bed based on the heat transfer mechanism for packed bed proposed by Kunii and co-workers is presented. The time-dependent hydrogen absorption/desorption rate and pressure in the metal hydride vessel calculated by the model were compared with the experimental results. During the hydriding, calculated hydrogen absorption rates agreed with measured ones. Calculated thermal equilibrium hydrogen pressures were slightly lower than the measured hydrogen pressures at the inlet of metal hydride vessel. Taking account of the pressure gradient between the inlet of metal hydride vessel and the metal hydride bed, it is considered that this discrepancy is reasonable. During the dehydriding, there were big differences between the calculated hydrogen desorption rates and measured ones. As calculated hydrogen desorption rates were lower than measured ones, there were big differences between the calculated thermal equilibrium hydrogen pressures and the measured hydrogen pressures at the inlet of metal hydride vessel. It is considered that those differences are due to the differences of the heat transfer characteristics such as thermal conductivity of metal hydride particles and porosity between the assumed and actual ones. It is important to obtain the heat transfer characteristics such as thermal conductivity of metal hydride particles and porosity both during the hydriding and dehydriding to design a metal hydride vessel.

Keywords: Metal hydride; Metal hydride vessel; Heat transfer; Energy storage

1. Introduction

Energy storage can play an important role in the operation of electric energy systems ranging from load leveling [1] to enabling the use of intermittent renewable energy sources such as wind or solar energy for remote sites to provide power on demand [2]. Energy storage system constructed around hydrogen is the combination of water electrolyzer, fuel cell and hydrogen-storage device. Using a water electrolyzer, electricity production in excess of demand is converted to hydrogen. Electricity demand in excess of production is met by converting hydrogen to electricity through a fuel cell. There are three basic methods for storing hydrogen: (1) compressed gas; (2) liquid; and (3) chemically bound (such as metal hydrides).

When using the metal hydrides, hydrogen-storage densities greater than those achieved by liquefaction are possible with gas pressures of just 0.1 or 0.2 MPa. The use of metal hydrides also offers potential safety advantages over the compressed hydrogen or liquefied hydrogen. A ruptured vessel of compressed hydrogen or liquefied hydrogen presents an immediate and serious hazard. If the vessel ruptured while in use, removal of the heat source driving the thermal decomposition should cause the reaction to quench itself. In addition, most metal hydrides do not react violently with air or water.

An α-phase solid solution reacts with a hydrogen to form β-phase hydride as shown:

$$\alpha\text{-phase (solid)} + \text{hydrogen (gas)} \leftrightarrow \beta\text{-phase (solid)} \quad (1)$$

The hydriding reaction is normally exothermic when it is proceeding to the right. On the other hand, the dehydriding reaction is endothermic when it is proceeding to the left. The performance of hydrogen absorption to and desorption from metal hydride vessel depends on the heat transfer, mass transfer and reaction kinetics of metal hydride bed. After a few hydriding and dehydriding cycles, metal hydride

* Corresponding author. Tel.: +81-78-9926527; fax: +81-78-9926510.
E-mail address: t.oi@pantec.co.jp (T. Oi).

0378-7753/$ – see front matter © 2003 Elsevier B.V. All rights reserved.
doi:10.1016/S0378-7753(03)00822-X

Nomenclature

d_f	pitch of fins (m)
d_p	diameter of metal hydride particles (m)
h^*	contact heat transfer coefficient between the metal hydride particles ($W m^{-2} K^{-1}$)
h_{MH}	overall heat transfer coefficient of the metal hydride bed ($W m^{-2} K^{-1}$)
h_{rs}	thermal radiative heat transfer coefficient between the metal hydride particles ($W m^{-2} K^{-1}$)
h_{rv}	thermal radiative heat transfer coefficient between the vacant spaces ($W m^{-2} K^{-1}$)
h_w	apparent heat transfer coefficient in the vicinity of bed's wall ($W m^{-2} K^{-1}$)
j	j factor
k_e	effective thermal conductivity of metal hydride bed accompanied with the hydrogen flow ($W m^{-1} K^{-1}$)
k_{e0}	effective thermal conductivity of metal hydride bed ($W m^{-1} K^{-1}$)
k_{ew0}	effective thermal conductivity in the region of $d_p/2$ from the inner surface of bed's wall ($W m^{-1} K^{-1}$)
k_f	thermal conductivity of hydrogen ($W m^{-1} K^{-1}$)
k_s	thermal conductivity of metal hydride particles ($W m^{-1} K^{-1}$)
L_1	spacing between the particle layers (m)
L_2	thickness of the vacant space (m)
L_3	thickness of the particle layer (m)
Pr	Prandtl number
Q_1	heat transfer rate through the hydrogen phase ($W m^{-2}$)
Q_2	heat transfer rate through the metal hydride phase–hydrogen phase–metal hydride phase ($W m^{-2}$)
Re	Reynolds number
ΔT	temperature difference (K)
Δx	distance between the center of solid layers (m)
X	hydrogen content (number of hydrogen atom/number of metal atom)

Greek letters

α	coefficient
β	coefficient
γ	coefficient
δ	coefficient
ϕ_1	porosity in the case where spheres are packed loosely
ϕ_2	porosity in the case where spheres are packed most compactly
ϕ_v	porosity of metal hydride bed
ϕ_w	porosity of metal hydride bed in the vicinity of bed's wall

particles break down into fine particles of under the several 10 μm size. These fine particles are good because a large surface area enhances both the heat transfer and mass transfer. However, fine particles leads to excessive pressure drop which reduces the mass transfer and to small effective thermal conductivity of metal hydride beds which reduces the heat transfer. Murthy and Gopal reviewed the state-of-the-art on heat and mass transfer in the metal hydride beds [3].

Experimental and theoretical studies of effective thermal conductivity in metal hydride beds have been carried out [4–9]. Pons and Dantzer demonstrated that small diameters of metal hydride powders (1–40 μm) are responsible for the low effective thermal conductivity values because of Knudsen effect [10]. They also pointed out that the wall heat transfer coefficient is an important parameter for characterizing and optimizing the heat transfer efficiency of metal hydride bed [11].

Different attempts to improve the effective thermal conductivity of metal hydride beds have been made: insertion of aluminum foam [12], integration of copper wire net structure [13], packing in a multilayer waved sheet structure [6], microencapsulated metal hydride compact [14], and compacting metal hydride powder with an expanded graphite [15].

For effective design of metal hydride vessel, a mathematical model is needed which effectively describes the physical and chemical process in a metal hydride bed. A number of pertinent and effective mathematical models for the process have been discussed [16–23].

Metal hydride vessels have been designed and manufactured [12,24,25]. The structure of almost vessels was based on the tubular type heat exchanger. In this paper, heat transfer characteristics of the metal hydride vessel based on the plate-fin type heat exchanger was investigated. A model is presented which describes heat transfer mechanism in the metal hydride bed based on the plate-fin type heat exchanger. The time-dependent hydrogen transfer rate and pressure in the metal hydride bed calculated by the model are compared with the experimental results. From the results of those comparison, the rationality and applicability of the employed model is discussed to design a metal hydride vessel.

2. Experimental procedure

2.1. Hydrogen-storage alloy

Hydrogen-storage alloys are broadly classified into three types according to the crystal structure and composition. The first one is AB_5 type hydrogen-storage alloy represented by $LaNi_5$. The second one is AB type hydrogen-storage alloy represented by TiFe. The third one is AB_2 type hydrogen-storage alloy represented by $TiCr_2$, $TiMn_{1.5}$ and one having C14 Laves structure. The beds in the metal hydride vessel were filled with AB_2 type hydrogen-storage alloy's particles, $Ti_{0.42}Zr_{0.58}Cr_{0.78}Fe_{0.57}Ni_{0.2}Mn_{0.39}Cu_{0.03}$, with a storage capacity of 0.92 wt.%. In this hydrogen-storage

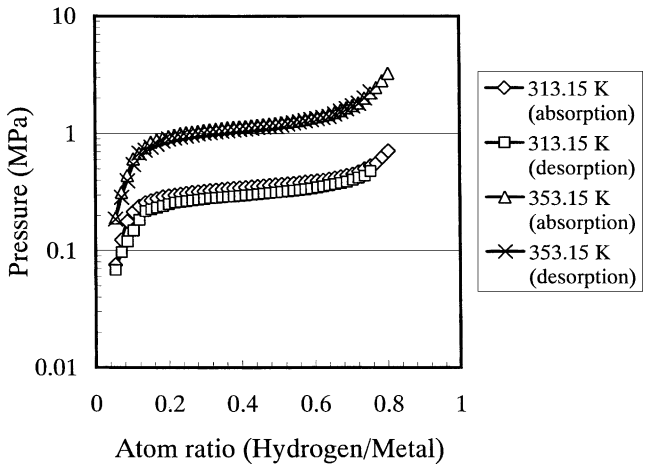

Fig. 1. Pressure–composition temperature diagram of $Ti_{0.42}Zr_{0.58}Cr_{0.78}Fe_{0.57}Ni_{0.2}Mn_{0.39}Cu_{0.03}$.

alloy, Zr is substituted for a part of Ti, and Fe, Ni, Mn and Cu are substituted for a part of Cr on the basis of $TiCr_2$. Each substituted element has the following effects [26]:

(1) Equilibrium plateau pressures become variable by the contents of substituted Zr and Fe.
(2) Fe increases hydrogen-storage capacity.
(3) Fe makes the beginning point of "plateau region" more distinct.
(4) Mn and Cu make the gradient of "plateau region" smaller.
(5) Mn, Ni and Cu make the hysteresis between the hydriding process and dehydriding process smaller.

A pressure–composition temperature diagram of this hydrogen-storage alloy is shown in Fig. 1. Absorption and desorption pressure plateau of the examined metal hydride are 0.37 and 0.31 MPa at the hydrogen/metal ratio of 0.5 and the temperature of 313.15 K, respectively.

2.2. Metal hydride vessel

The hydriding reaction in the metal hydride is exothermic. On the other hand, the dehydriding reaction is endothermic. Under hydriding/dehydriding reactions, the metal hydride beds must be heated or cooled. For this reason, the structure of the metal hydride vessel is the same as that of the heat exchanger.

In general, owing to the fine particles of metal hydride, the effective thermal conductivity of metal hydride bed usually has a value around $1\,W\,m^{-1}\,K^{-1}$ at the ambient temperature. Thus, the heat transfer resistance of metal hydride bed determines the overall heat transfer resistance in the case where liquid is used to heat and cool the metal hydride beds.

The methods suggested for heat and mass transfer enhancement can be broadly divided into two main groups. In the first method, the heat transfer effectiveness of the metal hydride bed is improved by providing extended area for heat transfer in the forms of fins, foams or meshes. Metal hydride particles are distributed into the matrix formed by the high thermal conductivity materials such as copper or aluminum. In the second method of enhancement, the metal hydride particles are consolidated through a binder or metal hydride particle. High thermal conductivity materials such as copper or carbon are compressed under high pressure into porous metal matrix hydride compacts.

The first method by fins was applied in this research. An exterior view of the metal hydride vessel is shown in Fig. 2. The cross-sectional view is shown in Fig. 3. Specifications are shown in Table 1. The concept of brazed plate-fin type heat exchanger was applied to extend the heat transfer area between the metal hydride particles and water. The vessel was composed of an aluminum alloy rectangular body and includes three packed beds for the metal hydride particles and four passages for the water. The metal hydride particles were filled between the fins.

2.3. Experimental setup

The measurements for the heat transfer characteristics of metal hydride vessel were performed using the experimental setup shown schematically in Fig. 4. Metal hydride vessel was provided with hydrogen from a high-pressure cylinder sold at a market. Hydrogen in a high-pressure cylinder was a byproduct from sodium chloride electrolysis, which was compressed, purified and filled up. Purity and dew point of hydrogen was 99.998% and 213.15 K, respectively. Impurity was nitrogen of which concentration was 19.3 ppm (0.00193 vol.%).

After maintaining the metal hydride vessel at the temperature and pressure of experimental conditions, hydrogen was absorbed into the metal hydride vessel or desorbed from the metal hydride vessel. The hydrogen flow rate was kept constant at 2.1 or $3.3\,N\,m^3\,h^{-1}$. Water of 0.6 or $1.2\,m^3\,h^{-1}$ was delivered to the vessel to remove or provide the reaction heat. The temperature distribution in the metal hydride bed, water inlet and outlet temperature, hydrogen pressure at the

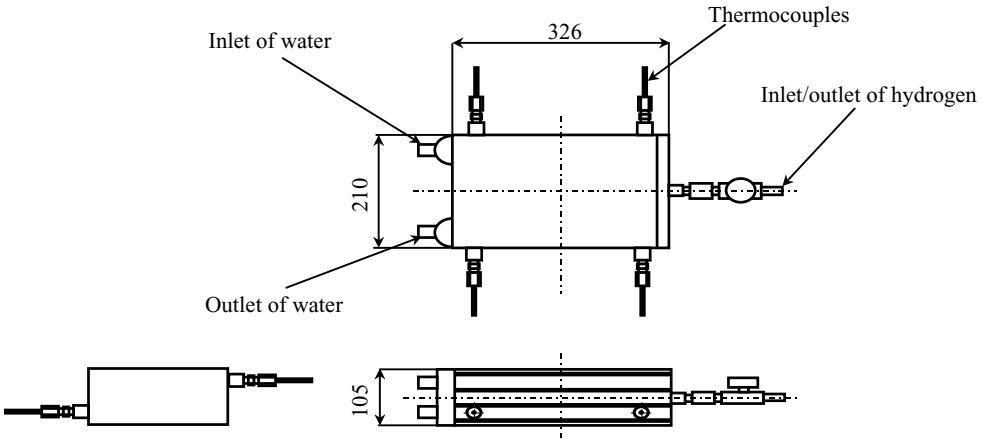

Fig. 2. Exterior view of the metal hydride vessel.

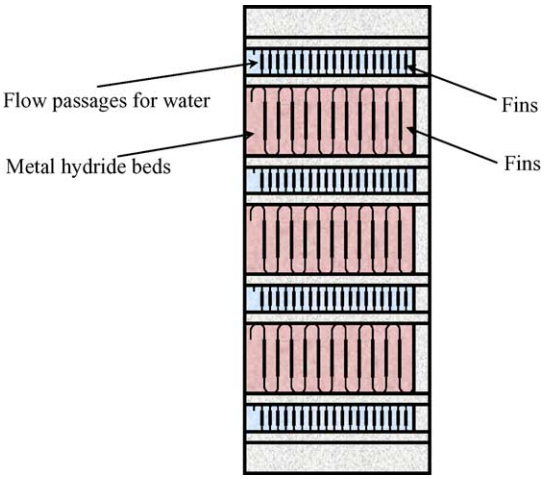

Fig. 3. Cross-sectional view of the metal hydride vessel.

Table 1
Specifications of the metal hydride vessel

Material	
Hydrogen-storage alloy	$Ti_{0.42}Zr_{0.58}Cr_{0.78}Fe_{0.57}Ni_{0.2}Mn_{0.39}Cu_{0.03}$
Vessel	Aluminum alloy
Storage capacity of hydrogen ($N\,m^3$)	>1
Weight (kg)	
Hydrogen-storage alloy	11.3
Vessel	19.7
Total	31
Overall size (mm)	
Height	105
Length	210
Width	326
Heat transfer area (m^2)	
Metal hydride beds	2.85
Flow passages for water	0.81

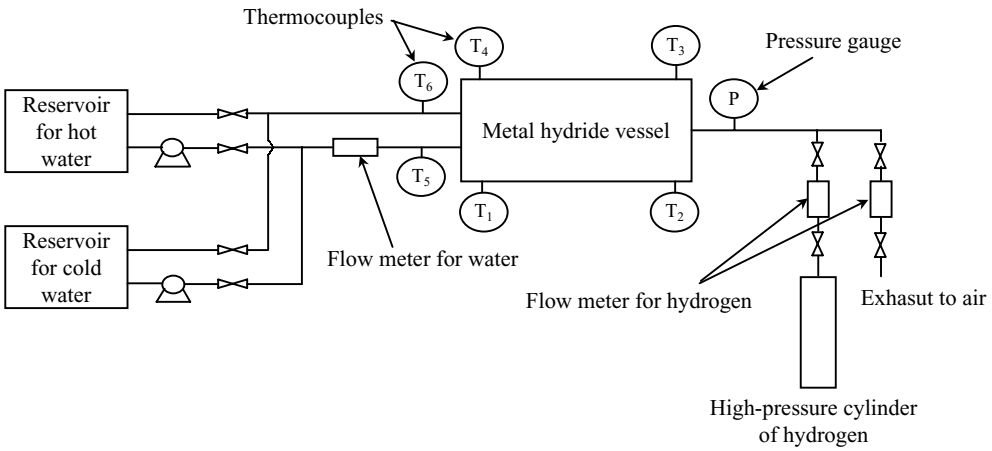

Fig. 4. Experimental setup.

inlet of metal hydride vessel, hydrogen flow rate and water flow rate were gathered using data acquisition equipment.

3. Heat transfer mechanism in the metal hydride bed

It can be considered that heat transfer mechanism in the metal hydride bed is the same as that in the common powder packed bed such as catalyst bed. Kunii and co-workers discussed the heat transfer mechanism in packed bed using the effective thermal conductivity in packed bed and apparent heat transfer coefficient in the vicinity of vessel's wall [27–30]. With reference to those discussions heat transfer mechanism in the metal hydride bed can be described as follows, provided that the following assumptions are made:

(1) The metal hydride particles and hydrogen in the vacancy of metal hydride bed are in thermal equilibrium.
(2) There is no pressure gradient within the metal hydride bed.
(3) The temperature in the metal hydride bed is only a function of time.

3.1. Effective thermal conductivity in the metal hydride bed

Yagi and Kunii gave an effective thermal conductivity in the packed bed accompanied with the fluid flow as follows [27]:

$$\frac{k_e}{k_f} = \frac{k_{e0}}{k_f} + \alpha\, Pr\, Re \tag{2}$$

As reactions in the metal hydride bed is usually fast, it can be considered that there is not hydrogen flow in the metal hydride bed. Even though the whole quantity of hydrogen introduced to or discharged from the vessel does not react, Reynolds number based on the diameter of metal hydride particles is very small. Thus, it can be considered that metal hydride bed is not accompanied with the hydrogen flow.

Heats are transferred in parallel by the following mechanisms in the case where temperature gradient exists in the metal hydride bed as shown in Fig. 5:

(1) Contact heat transfer between the metal hydride particles.
(2) Heat conduction through the thin hydrogen film in the vicinity of the contact point of metal hydride particles.
(3) Heat radiation from the surface to other surfaces of the metal hydride particles.
(4) Heat conduction through the metal hydride particles.
(5) Heat conduction through the hydrogen in a vacant space.
(6) Heat radiation from the vacant space to the adjacent another vacant space.

Heat transfer mechanism is modeled as shown in Fig. 6. Heat transfer rate through the hydrogen phase per unit area is described as follows:

$$Q_1 = \left(\frac{k_f}{L_1} + h_{rv}\right)\Delta T \tag{3}$$

Heat transfer rate through the metal hydride phase–hydrogen phase–metal hydride phase per unit area is described as follows:

$$Q_2 = \frac{\Delta T}{(1/(h^* + (k_f/L_2) + h_{rs})) + (L_3/k_s)} \tag{4}$$

It can be considered that heat between the metal hydride particles, vacant spaces and metal hydride particles is transmitted through the cross-sectional area of metal hydride bed equivalent to $1-\phi_v$. On the other hand, it can be considered that that between the vacant spaces is transferred through the cross-sectional area of metal hydride bed equivalent to ϕ_v. Temperature gradient between the surfaces C and D in Fig. 6 is $\Delta T/L_1$. Effective thermal conductivity that can describe the total heat transfer in the metal hydride bed is

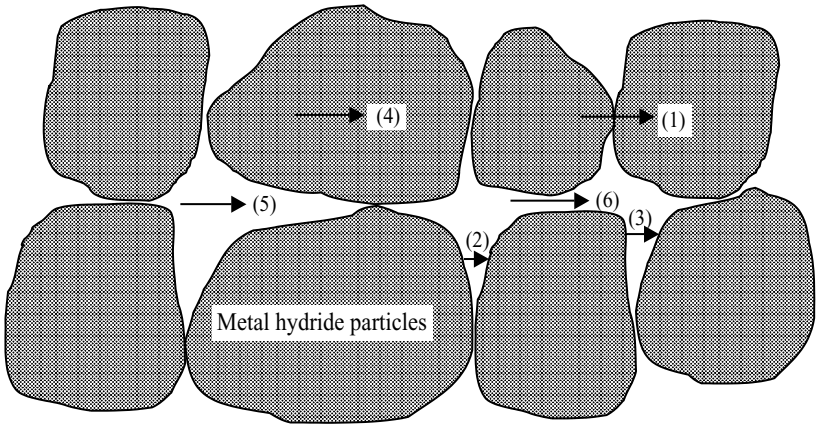

Fig. 5. Heat transfer in the metal hydride bed.

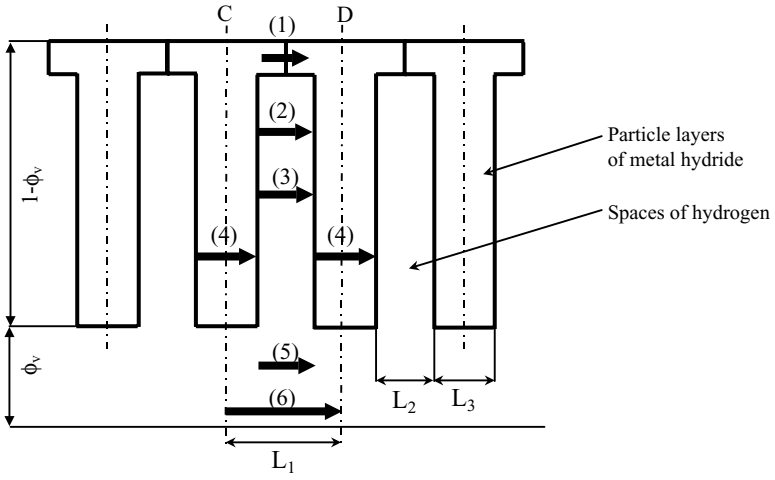

Fig. 6. Model for heat transfer in the metal hydride bed.

introduced as follows:

$$k_{e0}\frac{\Delta T}{L_1} = \phi_v\left(\frac{k_f}{L_1} + h_{rv}\right)\Delta T + \frac{(1-\phi_v)\Delta T}{(1/(h^* + (k_f/L_2) + h_{rs})) + (L_3/k_s)} \quad (5)$$

L_1 can be considered as the average distance between the centers of adjacent two metal hydride particles and is described as follows:

$$L_1 = \beta d_p \quad (6)$$

L_2 and L_3 are described, respectively, as follows:

$$L_2 = \gamma d_p \quad (7)$$

$$L_3 = \delta d_p \quad (8)$$

Substituting Eqs. (6)–(8) into Eq. (5), effective thermal conductivity of the metal hydride bed is described as follows:

$$\frac{k_{e0}}{k_f} = \phi_v\left(1 + \beta\frac{h_{rv}d_p}{k_f}\right) + \frac{1-\phi_v}{(1/((\beta/\gamma) + (\beta d_p/k_f)(h^* + h_{rs}))) + (\delta/\beta)(k_f/k_s)} \quad (9)$$

In the case where fluid exists in the vacant spaces of packed bed, contact heat transfer resistance between the particles is smaller than other heat transfer resistances and is negligible. When it is assumed that metal hydride particles are spheres of diameter d_p and particle layers in Fig. 6 are rectangular bodies of which cross-sectional area is $\pi d_p^2/4$ and volume is $\pi d_p^2/6$, δ is determined as 2/3. As the metal hydride bed investigated in this paper is operated around the ambient temperature, heat radiation is so small that this heat transfer mechanism is negligible. β is considered as 1. Therefore, effective thermal conductivity in the metal hydride bed is simplified as follows:

$$\frac{k_{e0}}{k_f} = \phi_v + \frac{1-\phi_v}{\gamma + (2/3)(k_f/k_s)} \quad (10)$$

γ gives the heat transfer rate through the fluid phase near the contact surface of solid particles. Kunii and Smith obtained γ of two cases [28]. First one is γ_1 for the case where spheres are packed loosely and porosity is 0.476. Second one is γ_2 for the case where spheres are packed most compactly and porosity is 0.26. It is supposed that actual packed bed may be a mixture of these two packing cases and γ in actual packed bed can be described as follows:

$$\gamma = \gamma_2 + (\gamma_1 - \gamma_2)\frac{\phi_v - \phi_2}{\phi_1 - \phi_2} = \gamma_2 + (\gamma_1 - \gamma_2)\frac{\phi_v - 0.26}{0.216} \quad (11)$$

3.2. Apparent heat transfer coefficient in the vicinity of bed's wall

Yagi and Kunii introduced an apparent heat transfer coefficient in the vicinity of tube's wall in the case where a fluid of high temperature is flowed into the packed bed and is cooled steadily by the tube's wall of constant temperature [29]. Shape of particles applied in their research was sphere. It was assumed that the ratio between the diameter of particles and inner diameter of tube was sufficiently small and the temperature difference between the fluid and particles was too small to be negligible. In this paper, those assumptions are applied.

It is assumed that temperature distribution in the metal hydride bed is determined by the effective thermal conductivity of metal hydride bed as described in Eq. (10). Using the effective thermal conductivity in the region of $d_p/2$ from the inner surface of bed's wall, apparent heat transfer coefficient in the vicinity of bed's wall is determined as follows:

$$\frac{h_w d_p}{k_f} = \frac{2}{(k_f/k_{ew0}) - (k_f/k_{e0})} \quad (12)$$

In the same manner as Eq. (9), effective thermal conductivity in the region of $d_p/2$ from the inner surface of bed's wall is described as follows:

$$\frac{k_{ew0}}{k_f} = \phi_w \left(2 + \frac{h_{rv} d_p}{k_f}\right) + \frac{1-\phi_w}{(1/((1/\gamma_w) + (h_{rs} d_p/k_f))) + (k_f/3k_s)} \quad (13)$$

As mentioned earlier, heat radiation is so small that this heat transfer mechanism is negligible. Therefore, Eq. (13) is simplified as follows:

$$\frac{k_{ew0}}{k_f} = 2\phi_w + \frac{1-\phi_w}{\gamma_w + (k_f/3k_s)} \quad (14)$$

γ_w is described as follows:

$$\gamma_w = \frac{((\kappa-1)/\kappa)^2}{4(\ln\kappa - ((\kappa-1)/\kappa))} - \frac{1}{3\kappa} \quad (15)$$

$$\kappa = \frac{k_s}{k_f} \quad (16)$$

3.3. Overall heat transfer coefficient of the metal hydride bed

Heat transfer resistance of the metal hydride bed is the sum of that of central part in the metal hydride bed and that in the vicinity of the bed's wall. Thus, overall heat transfer coefficient of the metal hydride bed is described as follows:

$$\frac{1}{h_{MH}} = \frac{d_f}{2k_{e0}} + \frac{1}{h_w} \quad (17)$$

4. Experimental results

Measurement results of time-dependent temperature of the metal hydride bed and pressure at the inlet of the metal hydride vessel during the hydriding at the inlet water temperature of 293.15 K and at the hydrogen flow rate of $3.3\,N\,m^3\,h^{-1}$ are shown in Fig. 7. Those during the dehydriding at the inlet water temperature of 313.15 K and at the hydrogen flow rate of $3.3\,N\,m^3\,h^{-1}$ are shown in Fig. 8. The difference of water flow rate does not influence on the

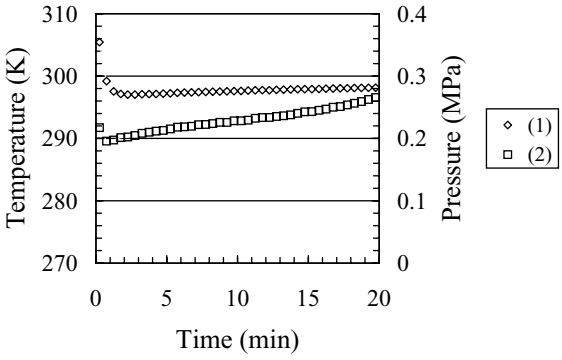

Water flow rate: 0.6 m^3h^{-1}
(1) Temperature of the metal hydride bed
(2) Pressure at the inlet of metal hydride vessel

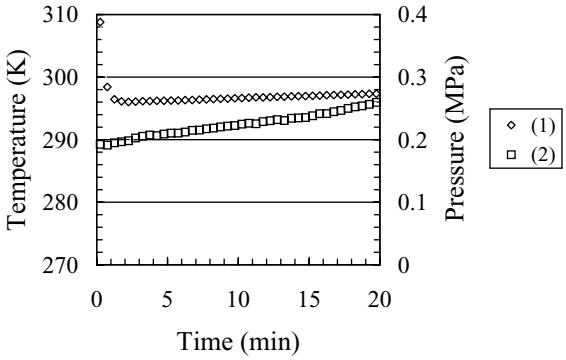

Water flow rate: 1.2 m^3h^{-1}
(1) Temperature of the metal hydride bed
(2) Pressure at the inlet of metal hydride vessel

Fig. 7. Measured results during the hydriding. Hydrogen flow rate, $3.3\,N\,m^3\,h^{-1}$; inlet water temperature, 293.15 K.

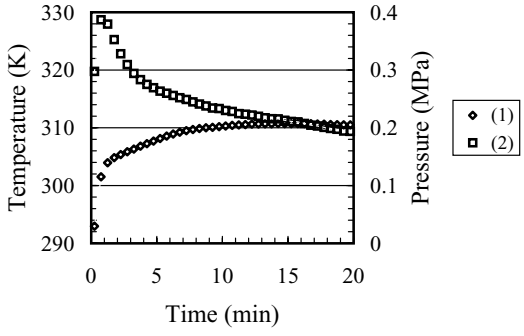

Water flow rate: 0.6 m^3h^{-1}
(1) Temperature of the metal hydride bed
(2) Pressure at the inlet of metal hydride vessel

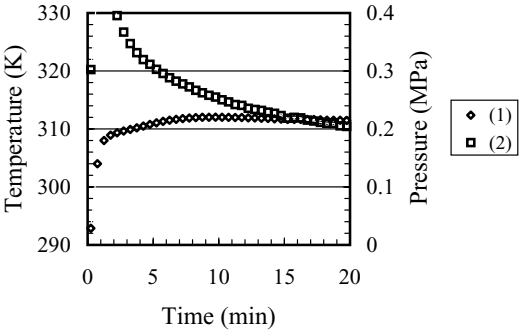

Water flow rate: 1.2 m^3h^{-1}
(1) Temperature of the metal hydride bed
(2) Pressure at the inlet of metal hydride vessel

Fig. 8. Measured results during the dehydriding. Hydrogen flow rate, $3.3\,N\,m^3\,h^{-1}$; water inlet temperature, 313.15 K.

metal hydride temperature and pressure at the inlet of the metal hydride vessel during both the hydriding and dehydriding. The effective thermal conductivity of metal hydride bed usually has a value around $1\,W\,m^{-1}\,K^{-1}$ at the ambient temperature. Thus, the difference of water flow rate does not influence on the overall heat transfer resistance of metal hydride bed.

5. Discussion

5.1. Dependences of effective thermal conductivity of metal hydride bed on thermal conductivity of metal hydride particles

Using these equations, calculated effective thermal conductivities of metal hydride bed at 293.15 K are shown in Fig. 9. Effective thermal conductivities of metal hydride bed increase with increase of thermal conductivity of metal hydride particles and with decrease of porosity of metal hydride bed. Generally, in the actual bed of uniform and small particles, porosity is in the range between 0.36 and 0.4 [30]. Measured effective thermal conductivity of metal hydride bed at the ambient temperature has a value around $1\,W\,m^{-1}\,K^{-1}$ [4,9]. When it is assumed that porosity of the metal hydride bed is 0.4 and thermal conductivity of metal hydride particles is in the range from 5 to $10\,W\,m^{-1}\,K^{-1}$, calculated effective thermal conductivities of metal hydride bed are almost equal to the measured results.

5.2. Comparison between the measured and calculated results

Calculated results of hydrogen flow rate absorbed to or desorbed from the metal hydride vessel and thermal equilibrium pressure are compared with the measurement results in order to verify the propriety of heat transfer mechanism in the metal hydride bed described in the earlier discussion as follows.

It is reported that the effective thermal conductivity of the metal hydride bed increases with the absorption of hydrogen. The large increase in effective thermal conductivity or decrease, respectively, in the plateau region is due to the large change of volume during absorption or desorption of hydrogen. So it is assumed that thermal conductivity of metal hydride particles is varied with the hydrogen content. Alloys based on titanium have thermal conductivity in the range of 7–15 $W\,m^{-1}\,K^{-1}$ at the ambient temperature [31]. With reference to those values, it was assumed that thermal conductivity of metal hydride particles was given by the following equation:

$$k_s = 3 + 5X \tag{18}$$

It was assumed that porosity of metal hydride bed was 0.4 [30] and that in the vicinity of bed's wall was 0.7 [29]. Heat transfer coefficient of water was calculated from the following equation:

$$j = 0.72Re^{-0.7} \tag{19}$$

Hydrogen content in the metal hydride vessel at the beginning of hydrogen absorption or desorption was determined using the measured temperature and pressure and the pressure–composition temperature diagram of metal hydride. Considering the enhancement of heat transfer by extended area of aluminum fins, temperature of vessel's wall, overall heat transfer coefficient of the metal hydride bed and heat transfer coefficient of water were determined so that heat transfer rate of metal hydride bed was equal to that of water. Heat transfer rate divided by the heat of hydriding reaction or that of dehydriding reaction gave hydrogen flow rate absorbed to or desorbed from the metal hydride vessel. Addition of increment of hydrogen content to or subtraction of reduction of hydrogen content from that of the previous time gave the hydrogen content at that time. Thermal equilibrium pressure of metal hydride bed at that time was determined using the measured temperature, obtained hydrogen content and pressure–composition temperature diagram of metal hydride.

Comparisons between the measured results and calculated ones during the hydriding and during the dehydriding are shown in Figs. 10 and 11, respectively. During the hydriding,

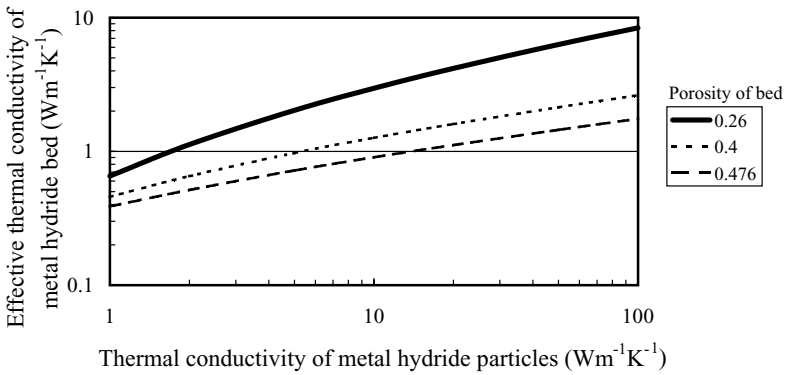

Fig. 9. Dependences of effective thermal conductivity of metal hydride bed on thermal conductivity of metal hydride particles.

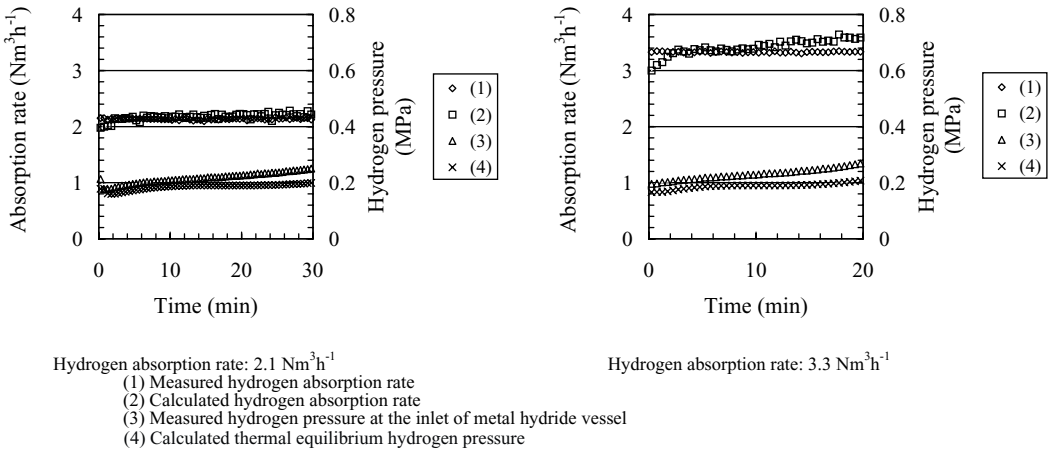

Fig. 10. Comparison between the measured results and calculated ones during the hydriding. Water flow rate, 0.6 $m^3\,h^{-1}$; inlet water temperature, 293.15 K.

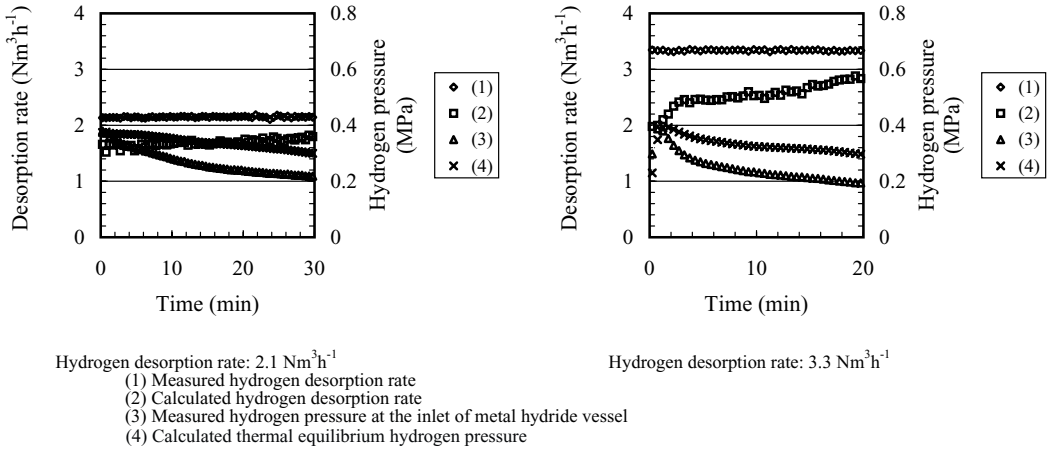

Fig. 11. Comparison between the measured results and calculated ones during the dehydriding. Water flow rate, 0.6 $m^3\,h^{-1}$; inlet water temperature, 313.15 K.

calculated hydrogen absorption rates agreed with measured ones. Calculated thermal equilibrium hydrogen pressures were slightly lower than the measured hydrogen pressures at the inlet of metal hydride vessel. Taking account of the pressure gradient between the inlet of metal hydride vessel and the metal hydride bed, it is considered that those discrepancies are reasonable.

In this paper, it is assumed that there are no differences of the heat transfer characteristics such as thermal conductivity of metal hydride particles and porosity between during the hydriding and during the dehydriding. However, for example, the effective thermal conductivity during the dehydriding is higher than that during the hydriding [9]. This hysteresis is probably due to the fact that the hydrogen content during the dehydriding is somewhat higher than during the hydriding at the same pressure. As a result, during the dehydriding there were big differences between the calculated hydrogen desorption rates and measured ones. As calculated hydrogen desorption rates were lower than measured ones, there were big differences between the calculated thermal equilibrium hydrogen pressure and the measured hydrogen pressure at the inlet of metal hydride vessel.

6. Conclusions

Heat transfer characteristics of the metal hydride vessel based on the plate-fin type heat exchanger were investigated. Calculated results using the heat transfer model in the metal hydride bed based on the heat transfer mechanism for packed bed proposed by Kunii and co-workers were compared with the measured results. During the hydriding, calculated hydrogen absorption rates agreed with measured ones. Calculated thermal equilibrium hydrogen pressures were slightly lower than the measured ones at the inlet of metal hydride vessel. Taking account of the pressure gradient between the inlet of metal hydride vessel and the metal hydride bed, it is considered that those discrepancies are reasonable.

There are differences of the heat transfer characteristics such as thermal conductivity of metal hydride particles and

porosity between during the hydriding and during the dehydriding. As a result during the dehydriding there were big differences between the calculated hydrogen desorption rates and measured ones. As calculated hydrogen desorption rates were lower than measured ones, there were big differences between the calculated thermal equilibrium hydrogen pressures and the measured ones at the inlet of metal hydride vessel.

It is important to obtain the heat transfer characteristics such as thermal conductivity of metal hydride particles and porosity both during the hydriding and dehydriding to design a metal hydride vessel.

References

[1] J. Kondoh, I. Ishii, H. Yamaguchi, A. Murata, K. Otani, K. Sakuta, N. Higuchi, S. Sekine, M. Kamimoto, Energy Convers. Manage. 41 (2000) 1863.
[2] S.R. Vosen, J.O. Keller, Int. J. Hydrogen Energy 24 (1999) 1139.
[3] S.S. Murthy, M.R. Gopal, J. Energy Heat Mass Transfer 18 (1996) 223.
[4] A. Yoshida, Y. Naka, T. Ohkita, Trans. JSME B 56 (1990) 536.
[5] D.W. Sun, S.J. Deng, Int. J. Hydrogen Energy 15 (1990) 331.
[6] D.W. Sun, S.J. Deng, J. Less Common Met. 160 (1990) 387.
[7] S. Suda, Y. Komazaki, J. Less Common Met. 172–174 (1991) 1130.
[8] J. Kapischke, J. Hapke, Exp. Therm. Fluid Sci. 17 (1998) 347.
[9] E. Hahne, J. Kallweit, Int. J. Hydrogen Energy 23 (1998) 107.
[10] M. Pons, P. Dantzer, J. Less Common Met. 172–174 (1991) 1147.
[11] M. Pons, P. Dantzer, J.J. Guilleminot, Int. J. Heat Mass Transfer 36 (1993) 2635.
[12] S. Lévesque, M. Ciureanu, R. Roberge, T. Motyka, Int. J. Hydrogen Energy 25 (2000) 1095.
[13] M. Nagel, Y. Komazaki, S. Suda, J. Less Common Met. 120 (1986) 35.
[14] K.J. Kim, G. Lloyd, A. Razani Jr., K.T. Feldman, Powder Technol. 99 (1998) 40.
[15] K.J. Kim, B. Montoya, A. Razani, K. Lee, Int. J. Hydrogen Energy 26 (2001) 609.
[16] A.V. Kuznetsov, K. Vafai, Int. J. Heat Mass Transfer 38 (1995) 2837.
[17] A. Jemni, S. Ben Nasrallah, Int. J. Hydrogen Energy 20 (1995) 43.
[18] A. Jemni, S. Ben Nasrallah, Int. J. Hydrogen Energy 20 (1995) 881.
[19] A. Jemni, S. Ben Nasrallah, Int. J. Hydrogen Energy 22 (1997) 67.
[20] A. Jemni, S. Ben Nasrallah, L. Jilani, Int. J. Hydrogen Energy 24 (1999) 631.
[21] T. Nakagawa, A. Inomata, H. Aoki, T. Miura, Int. J. Hydrogen Energy 25 (2000) 339.
[22] M. Mat, Y. Kaplan, Int. J. Hydrogen Energy 26 (2001) 957.
[23] K. Aldas, M. Mat, Y. Kaplan, Int. J. Hydrogen Energy 27 (2002) 1049.
[24] K. Nishimura, C. Inazumi, K. Oguro, I. Uehara, Y. Itoh, S. Fujitani, I. Yonezu, Int. J. Hydrogen Energy 25 (2000) 1087.
[25] W.H. Fleming, J.A. Khan, C.A. Rhodes, Int. J. Hydrogen Energy 26 (2001) 711.
[26] T. Kabutomori, T. Takahashi, H. Takeda, Y. Wakisaka, Nihonseikosyo Giho 53 (1997) 21.
[27] S. Yagi, D. Kunii, AIChE J. 3 (1957) 373.
[28] D. Kunii, J.M. Smith, AIChE J. 6 (1960) 71.
[29] S. Yagi, D. Kunii, Int. Dev. Heat Transfer Part IV (1962) 750.
[30] D. Kunii, M. Suzuki, Int. J. Heat Mass Transfer 10 (1967) 845.
[31] Y.S. Touloukian, R.W. Powell, C.Y. Ho, P.G. Klemens (Eds.), Thermophysical Properties of Matter, vol. 1, Plenum Press, New York, 1970, p. 1073.